

3D Modeling Approach of Fault Seal Integrity Analysis in Sonia Field Onshore Niger Delta

Oshodi D. Raymond^{1*} and John O. Amigun¹

¹Department of Geophysics, Federal University of Technology, Akure, Nigeria.

Authors' contributions

This work was carried out in collaboration between both authors. Both authors read and approved the final manuscript.

Article Information

Editor(s):

- (1) Dr. Xu Chong, Institute of Geology, China.
(2) Dr. Mohamed M. El Nady, Egyptian Petroleum Research Institute, Egypt.

Reviewers:

- (1) Myriam Patricia Martinez, Universidad Nacional de San Juan, Argentina.
(2) Fouad F. Shaaban, College of Basic Education, Kuwait.
(3) Sudad H. AL-Obaidi, Mining University, Russia.

Complete Peer review History: <https://www.sdiarticle4.com/review-history/74042>

Original Research Article

Received 28 July 2021
Accepted 05 October 2021
Published 12 October 2021

ABSTRACT

Geologic structures that aids the accumulation of hydrocarbon in reservoirs could be fault assisted or fault dependent, these faults can be described as sealing or leaking in nature. In this study, well logs and 3D seismic data were utilized for the seal integrity analysis in Sonia Field onshore Niger Delta.

The methods employed include reservoir evaluation (i.e. Determining the volume of shale), and the generation of 3D models by computing the fault seal algorithms such as the shale gouge ratio, which was used to access the sealing capacity of the fault planes trending NW-SE in the study area. In order to ascertain the sealing integrity of the identified hydrocarbon bearing sand, the following were done: horizon to fault intersection on the shale gouge ratio model, the 3D models of the fault attributes i.e. Fault-throw. Hydrocarbon column height (HCH and fault flow properties specifically, fault transmissibility and fault permeability using 'Manzocchi' equation.

The shale gouge ratio ranged from < 20% (leaking zones) to ≥ 60% (sealing Zones) across the fault plane. The hydrocarbon column height at which the faults in the study area can support ranges between 26.6 m to 28.0 m. The predicted permeability model of the faults is less than 1mD in some regions along the fault plane with corresponding transmissibility values between 0 and 0.20. Based on these results, it was observed that none of the hydrocarbon reservoirs in the study area falls

*Corresponding author: E-mail: oshodiraymond@gmail.com;

within in the leaking category. The fault permeability and transmissibility models which indicate that regions along the faults planes are sealed and might prevent migration of fluid out of these reservoirs.

Keywords: Faults; Shale Gouge Ratio; hydrocarbon column height; fault transmissibility; fault permeability.

1. INTRODUCTION

In hydrocarbon exploration and production, faults can act as pathways or barricades for the migration of hydrocarbon. The existence of faults increases the risks for hydrocarbon exploration and development [1]. In the subsurface, faults can trap fluids such as hydrocarbon and water; hence, they are of economic importance. During hydrocarbon exploration, determining the sealing capacity of faults can influence the assessment of the likelihood of finding hydrocarbons and the estimate of the likely resource range [2].

Faults and their behaviors needs to be understood by geologist and engineers in-order to effectively explore and extract hydrocarbon reserves [3]. However, Juxtapositions seal and fault rock seal are the types of fault seal. Juxtaposition seal refers to a situation whereby reservoir unit and non-reservoir unit (low permeability unit) are positioned side by side .While, the fault rock seal refers to some type of smearing or gouge that has been incorporated into the fault zones causing a low permeability barrier. Consequently, seal integrity analysis has been simplified by well-grounded algorithms which gives a means to appropriately estimate the sealing capacity of faults. Hence, the way fault behaves in siliclastic sequence can be adequately represented and quantified with the aid of these algorithms [4].

Therefore ,modern algorithms such as Shale Gouge Ratio (SGR), Shale Smear Factor (SSF), and Shale Smear Potential (SSP), have been utilized in predicting the quantity of fine-grained (phyllosilicate) material that can act as a low permeability barrier within a fault zone [5]. These algorithms can then be utilized as an input in generating the capillary threshold pressures [6,7] that the fault planes can support [8].

The fault flow properties that needs to be considered during a production simulation are permeability and transmissibility. They form the basis for understanding the reservoir communication across the fault planes. Hence, reservoir characterization have been done in so many fields in Niger Delta [9-11]. But seal integrity assessment is not common, it is a

breach that needs to be filled in order to enhance oil recovery and boost reserve portfolio. Furthermore, fault seal integrity assessment is crucial particularly in regions that are structurally controlled. Ignoring seal integrity assessment and depending merely on reservoir parameters can result in an unequal division of oil reserves. This study was aimed to evaluate seal integrity of the faults in Sonia field onshore Niger-Delta. The objectives of this research work includes: identification of structural traps, generating 3D models of the fault throw distributions, shale gouge ratio and hydrocarbon column height, fault permeability and transmissibility.

2. LOCATION AND GEOLOGY OF THE STUDY AREA

Sonia field is an onshore field located in the western region of the Niger Delta Basin (Fig. 1). The basin in Niger Delta is situated at the North Eastern margin of the Gulf of Guinea on the West coast of Africa, and it covers an area extent of about 75,000km² and it's at least 11km deep [12,13]. The Niger Delta comprises of three litho-stratigraphic units which are strongly diachronous [14 -16].

These litho-stratigraphic units in Fig. 2, from the oldest to the youngest consist of the Akata Formation which is made up of dark gray shales and silts with rare streaks of sand of possible turbidite flow source. This formation is projected to be 7000m thick in the central part [14]. This formation is made up of marine shales, which form the key source rocks for petroleum occurrence.

Agbada Formation spans through the Niger Delta clastic wedge and has at least a thickness over 3,000m [14]. This formation is the hydrocarbon-prospective sequence in the Niger Delta, where the sand serves as reservoirs and shale as the source rock, this formation is believed to have originated from the fluvial-deltaic environment, and Agbada Formation ranges from Eocene to Pleistocene in age [17].

The Benin Formation is basically the uppermost part of the Niger Delta [14] This Formation entails the recent subaerially exposed delta top surface.

The shallow portion of Benin Formation ranges from Oligocene to recent in age, and made up of non-marine sands that were deposited in either upper coastal plain or alluvial depositional environments [12,13].

The sedimentary wedge in Niger Delta has been grouped into in five depobelts, these includes: Greater Ughelli, Central Swamp, Northern Delta, Coastal Swamp, and Offshore depobelts [14,18]. The area of study lies at the western part of the Coastal Swamp depo-belt. This depobelt is characterized by continental slope, linked with growth faults, rollover anticlines and collapsed crests [18,19].

3. MATERIALS AND METHODS

The data set used for this study includes three dimensional seismic data in SGY format and suites of wireline logs from five wells (concentrated principally at the central part of the field). The seismic volume contains a total number of 883 in-lines and 762 cross-lines. The suit of wireline logs comprises of gamma ray log, resistivity log, density log, neutron log, and check-shot data. The check-shot data was used in converting the time values to depth and to carry out well to seismic tie. The procedure used to accomplish the desired task is presented in the flowchart in Fig. 3.

The reservoirs were delineated from the sand units that showed high resistivity values, these sand units were correlated across the wells, their respective horizons were mapped on the seismic section. The faults were identified by looking for displacements, polarity reversal and changes in seismic facies the fault interpretation was quality controlled by monitoring the consistency of the mapped faults on the 3D window in Petrel™ 2017 software version, these faults were modeled and fault polygons were generated by synchronizing the faults with the mapped horizons.

In order to determine the sealing capacity of the identified reservoirs in the study area, the analysis carried out include: horizon to fault intersection, volume of shale, fault bed thickness, throw estimation, generation of juxtaposition maps, Shale Gouge Ratio (SGR), and Hydrocarbon Column Height (HCH) in order to predict the probable height of hydrocarbon the faults in the study area can support. Finally, the fault flow properties i.e. fault permeability and fault transmissibility were determined using “Manzocchi” 1999 empirical equations.

3.1 Fault Seal Algorithms

Three dimensional models of the fault seal algorithm i.e. Shale Gouge Ratio were used to determine the sealing capacity of the faults. However, hydrocarbon column height models and the fault flow property models i.e. fault transmissibility and fault permeability were appropriately analyzed using the empirical equations in this section.

3.1.1 Shale Gouge Ratio

The SGR is for the prediction of the amount of clay or shale material in the fault zone. The higher the Shale Gouge Ratio (SGR), the greater the sealing potential of faults.

$$SGR = \frac{V_{sh} \times \Delta z}{t} \quad (1)$$

Where V_{sh} = volume of shale Δz = Bed Thickness
t = Throw

The global classification of fault based on SGR values <0.2 (20%) is associated with cataclastic fault gouge and the sealing capacity of this fault is considered to be unlikely [20,21].

A process whereby metamorphic rock is formed by continuous fracturing and comminution of existing rock is known as cataclasis, its mostly associated with fault zones during faulting, the reduction of solid minerals from average particle size to a smaller average particle size is referred to as comminution [21]. while SGR > 20% indicates a higher sealing potential. Furthermore, shale gouge ratio > 20% was further divided into three categories by [22].

- i) SGR from 20 to 40% (0.2-0.4) is associated with phyllosilicate framework and some clay smear fault rocks, here the fault is taken as poor seal and will be retarding to fluid flow.
- ii) SGR from 40-60%(0.4-0.6) fault is moderately sealed associated with mainly clay smears
- iii) SGR > 60 %(0.6) is taken as likely sealed fault zones.

3.1.2 Hydrocarbon Column Height

Fault zone capillary entry pressure (FZP) was linked to SGR based on equation (2)

$$FZP(\text{bar}) = 10^{(SGR/27-c)} \quad (2)$$

where: C is the lifting correction (ms).For burial depths less than 3.0 km (9850 ft) C = 0.5
 C = 0.25 for burial depths between 3.0 and 3.5 km(9850-11,500 ft),
 C = 0 for burial depth that is greater than 3.5 km (11,500 ft).

Since there is no core-data, for this study, the approach selected for this process required less input parameters than the other available options and therefore is prone to fewer errors in the computation of the hydrocarbon column height [23].

Hydrocarbon Column heights of the faults were estimated using fluid densities of 700 kg/m³ for oil, 1100 kg/m³ for water, and 0.5 was used for uplifting correction (C) since the deepest faults and horizons is less than 3.0km (9850 ft).

Hydrocarbon buoyancy was calculated using equation 3

$$pb = (\rho_w - \rho_h)gh \tag{3}$$

Since there is unavailability of pressure data in the course of this study, Seal threshold pressure was determined using the relationship of [24-27].

$$pc = \frac{2\gamma\cos\theta}{r} \tag{4}$$

$$H_{max} = \frac{pc}{g(\rho_w - \rho_h)} \tag{5}$$

Where Pc is the threshold pressure (Pascal (10⁵ Pa=1 bar)), γ is the surface tension (N/m), θ is the wetting angles, r is the pore throat radius (m), H_{max} = maximum hydrocarbon column height (m),

h = hydrocarbon column thickness in (ft)

ρ_w = water density(kg/m³),

ρ_h = hydrocarbon density (kg/m³),

g = acceleration due to gravity

$$H_{max} = \frac{FZP}{g(\rho_w - \rho_h)} \tag{8}$$

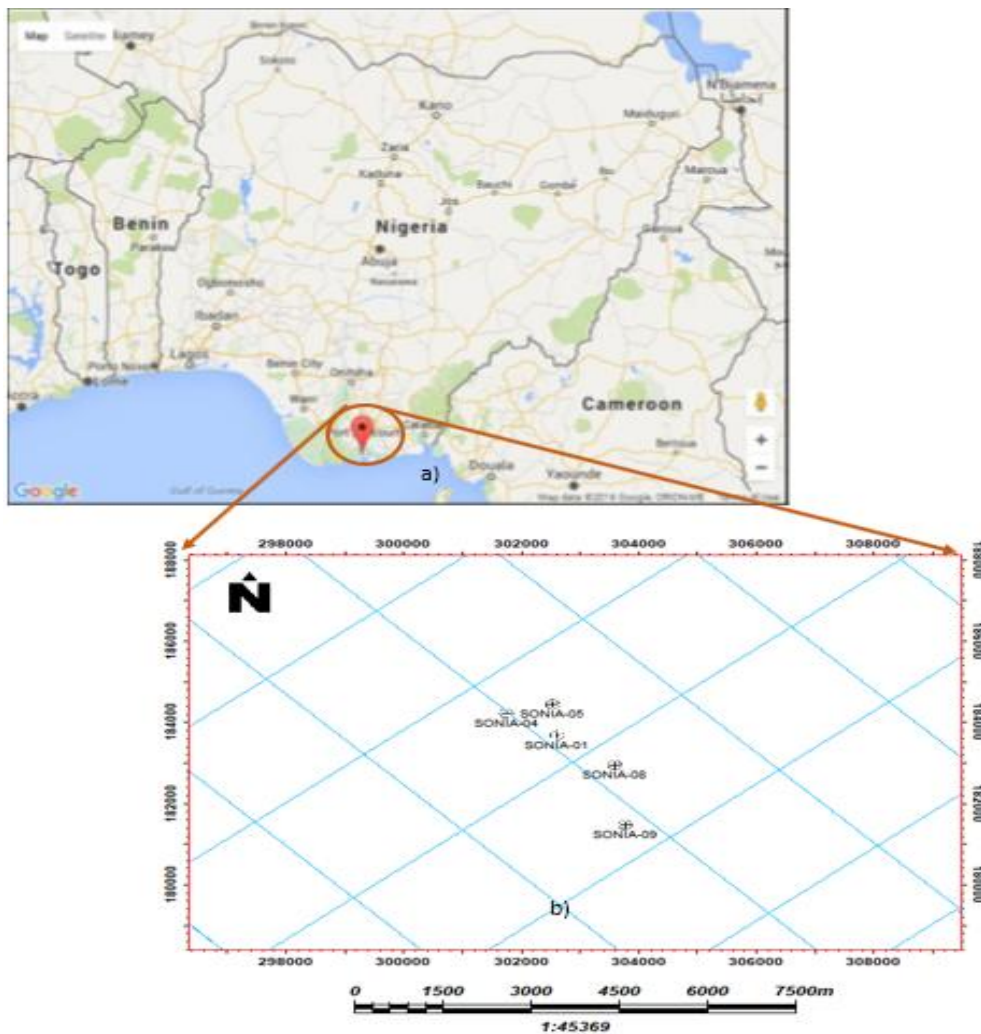


Fig. 1. Location of the Study area (b): Base-map of the study area showing the seismic Lines

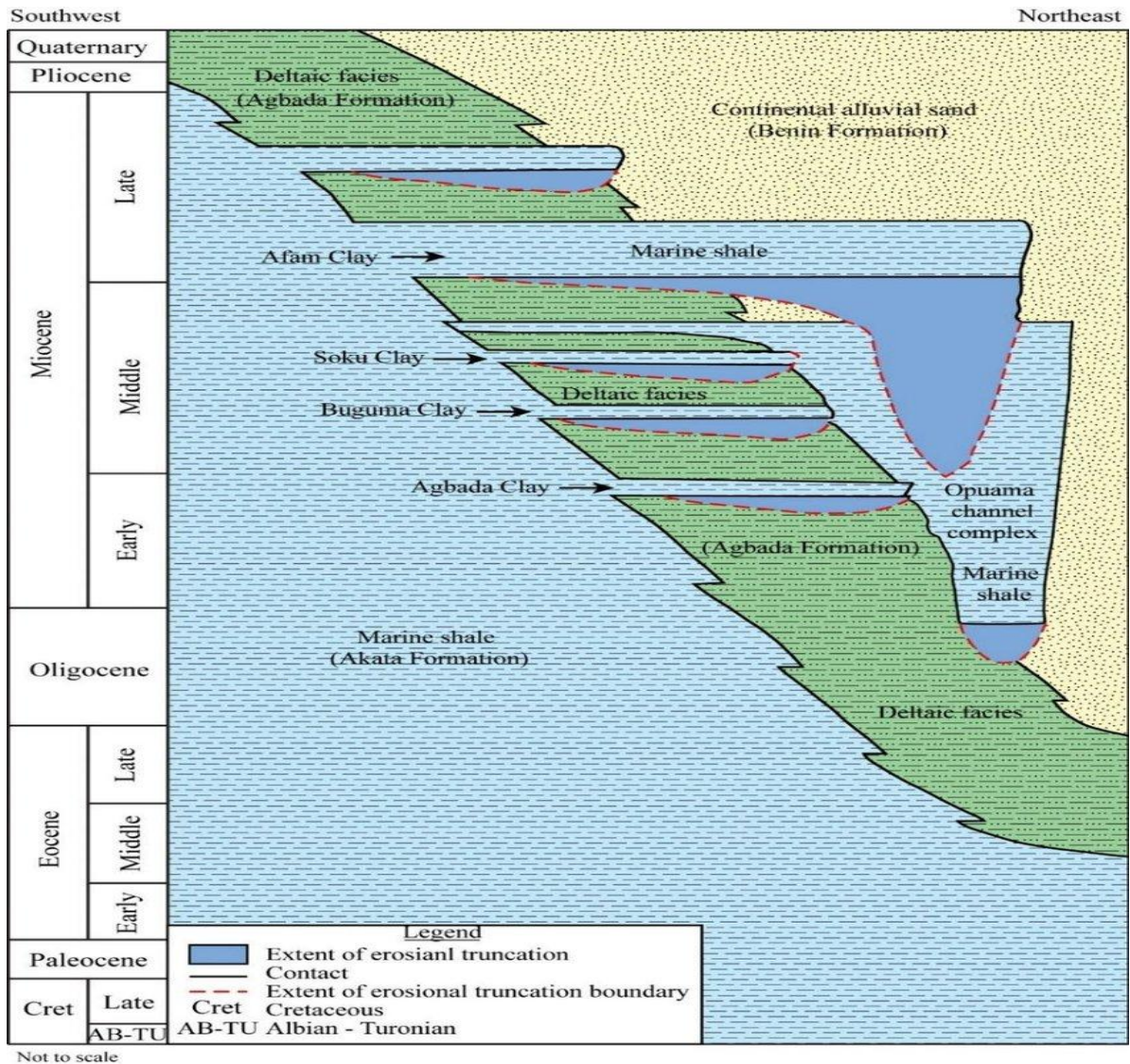


Fig. 2. Schematic cross section of the Niger-Delta showing the lithostratigraphic units [14]

3.1.3 Fault Flow Properties

Fault permeability is a property that describes the ease at which fluid flow [28] estimated using the equation stated below [29]

$$\log k_f = -4SGR - 1/4 \log(D) \times (1 - SGR)^5 \quad (9)$$

Where: k_f = Fault permeability
 D = Fault Displacement

For improved understanding of reservoir communication across the faults, the fault transmissibility multiplier distribution across the fault planes were determined, using the combination of predicted fault-rock permeability values and the fault thickness [29].

$$\text{Transmissibility} = \text{Fault Permeability} \times \text{Fault Rock Thickness} \quad (10)$$

$$\text{Fault Rock Thickness (Ft)} = \text{Displacement} / 66 \quad (11)$$

4. RESULTS AND DISCUSSION

4.1 Well Log Correlation and Seismic Interpretation

It is important to determine how laterally distributed the identified reservoir formations are within the subsurface. Therefore, four reservoirs (Res 1, Res 2, Res 3 and Res 4) as shown in Fig. 4 were correlated across the wells in Northwest - Southeast direction of the field. The correlation panel shows the gamma ray log on

the first track while the resistivity log is displayed on the second track, these logs were used to determine the hydrocarbon presence in a reservoir.

Low gamma ray signifies a sandstone formation while high resistivity value determines the presence of hydrocarbon in the formation. However, high gamma ray log implies a shale formation. The shale acts as a marker that seals the top and bottom of the reservoir. Furthermore, a total of 10 faults and four horizons were mapped on the Seismic section in Fig. 5 out of these mapped faults three are major faults interpreted as normal growth fault and the remaining faults are minor faults interpreted as antithetic faults in NW-SE strike orientation dipping south .

The structural traps in “Sonia” field are bounded by faults. “Faults can result in an effective hydrocarbon traps closed by an anticlinal structure [30]. The reflected events (i.e. horizons) identified on the seismic section were mapped on both the inline and crosslines. Eight horizons were mapped in total. i.e. four tops and their respective bases. The horizons were mapped in order to understand the structural frame workof the field and to identify closures within the seismic volume as shown in Fig. 5b.

At the completion of the seismic interpretation, the mapped horizons were used to generate the structural maps, the interpreted faults were modelled via Petrel 2017 software.

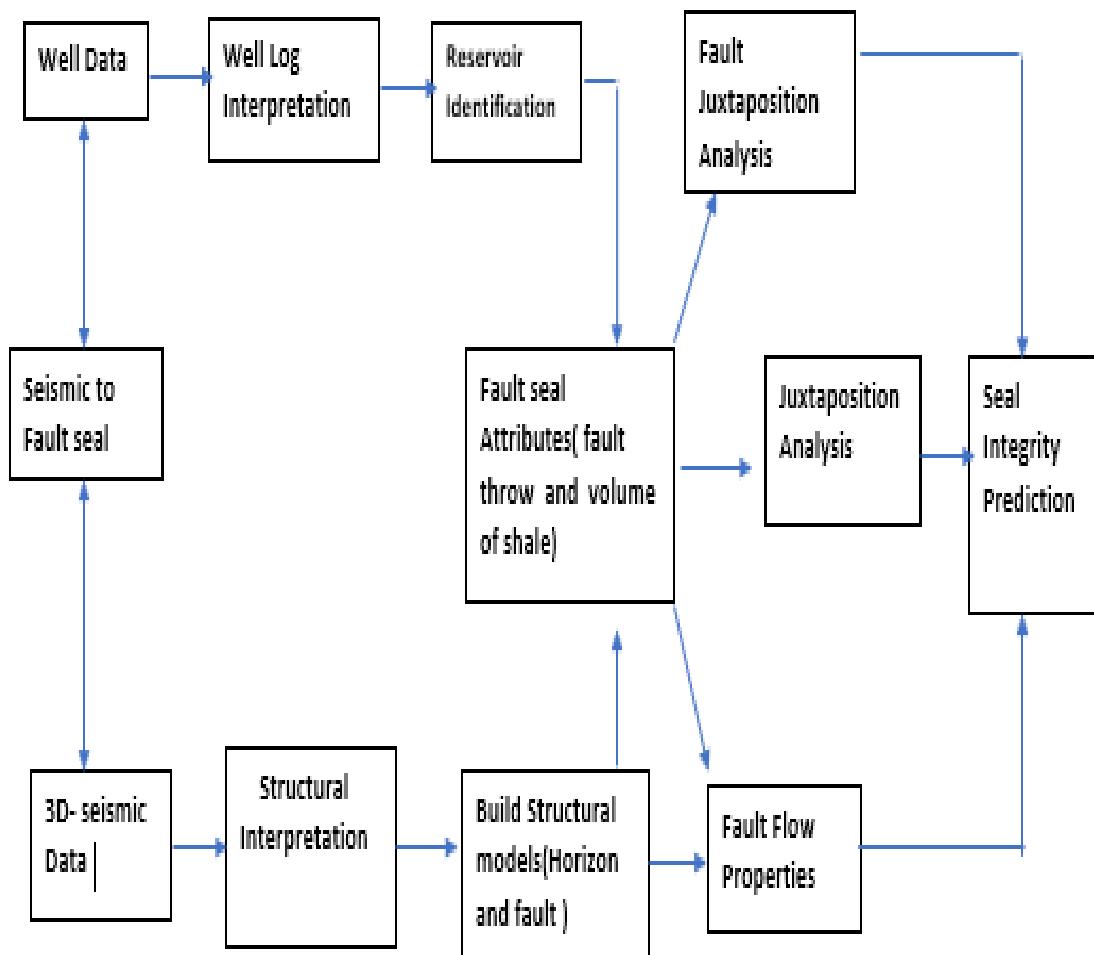


Fig. 3. Workflow Adopted for the Research Work

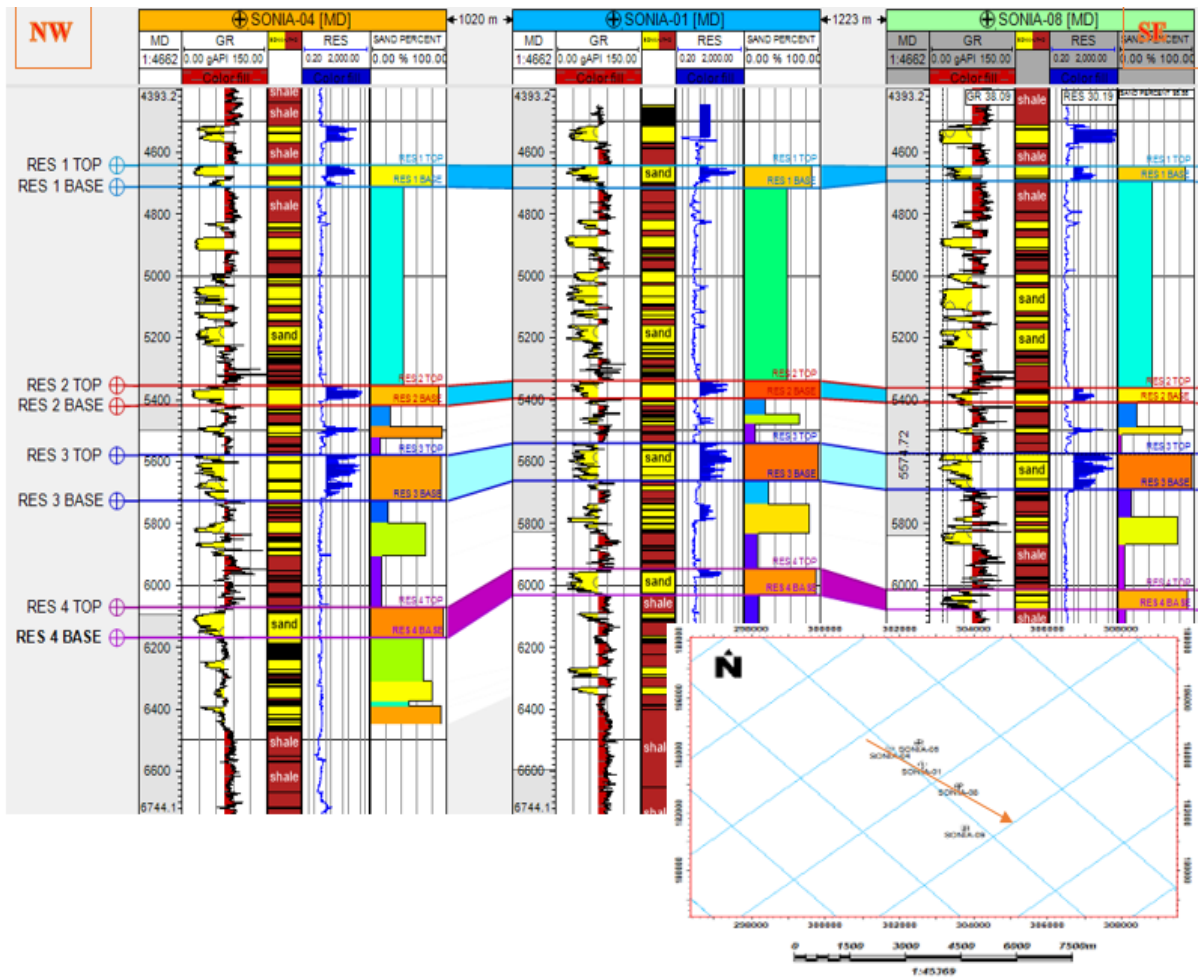


Fig. 4. Well Log Correlation Panels Across the Wells in the Study Area in NW-SE Direction

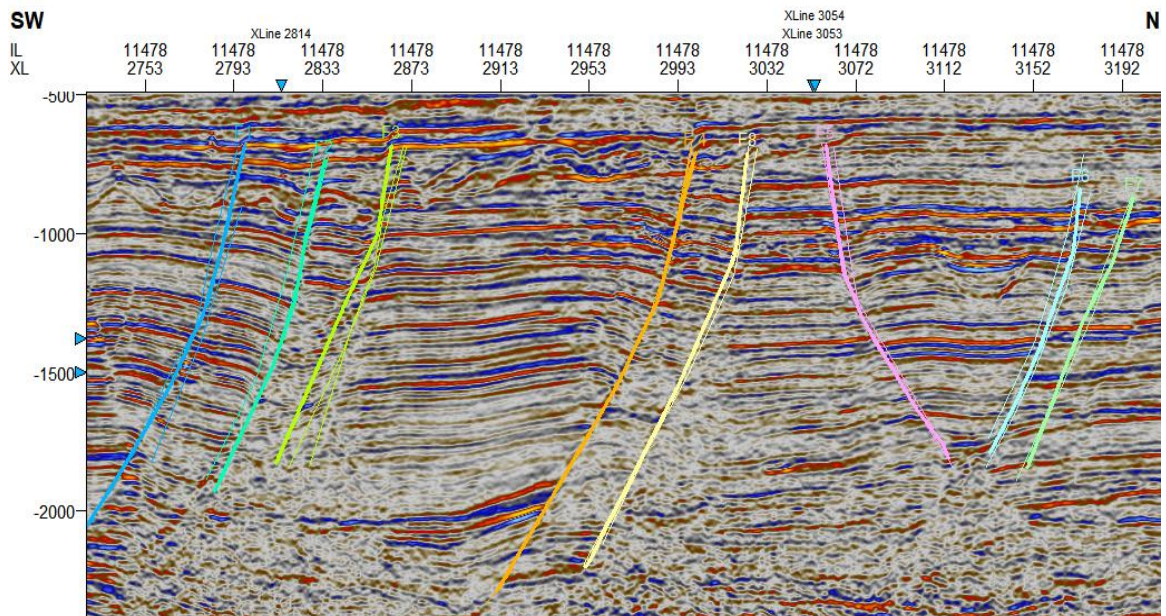


Fig. 5a. The Interpreted Faults in the Study Area

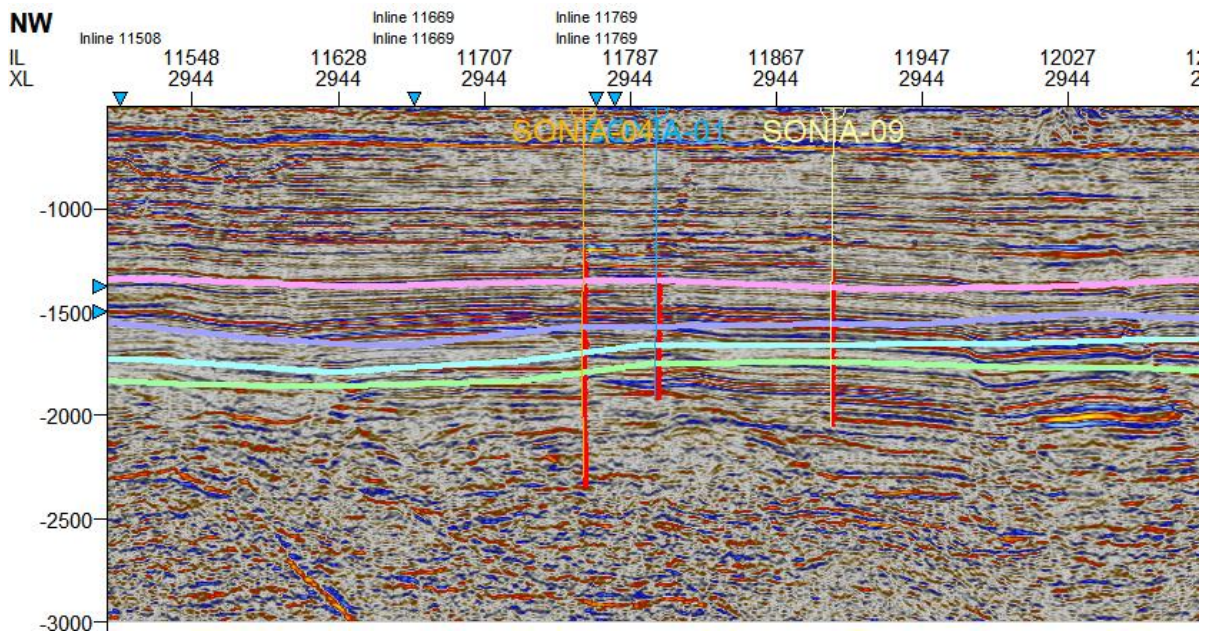


Fig. 5b. The Interpreted Horizons in the Study Area

Four depth structural maps were generated as shown in Fig. 7a to 7d by converting the time structure map to depth via the check shots velocity data. It's essential to generate depth maps because the drillers are interested in the depth at which the hydrocarbon can be extracted.

The plot of the depth against the two-way-travel time (TWT) was plotted such that the models gotten from the graph is used for time-to-depth conversion as indicated in Fig. 6. Each depth map depicts the depth to the top of each reservoir, close contours suggests structurally high regions (anticlines) which are traps for hydrocarbon accumulation. The anticlinal structure on these maps justifies the reason for drilling the producing five wells at the central region of the field, the anticlinal trap observed in the study area is bounded by faults F4 and F5. The structural analysis would be carried out on the fault dependent structure (structural trap) of "Sonia field".

4.2 Fault Sealing Analysis

A total of ten faults were mapped within the study area as shown on the structural maps. It is important to note that wells in study area are targeted between faults F4 and F5 at the central region of the field accompanied with a four way closure i.e. a roll over anticlinal structure.

Therefore, these faults were carefully analyzed, in order to ascertain the seal integrity of the

faults supporting the trap in this region and to determine whether or not hydrocarbons have migrated out of the trap. The fault sealing attributes encompasses the estimation of the fault throw and volume of shale, while the structural analysis of the faults involve the generation of maps and models, which include the juxtaposition map along the fault plane, shale gouge ratio (SGR), hydrocarbon column height and fault flow properties i.e. transmissibility and permeability.

4.2.1 Fault Throw Analysis

Fault throw distribution analysis along the fault planes is an effective method to quality check model intersection. The major contributor to the accumulation of hydrocarbon is the Hanging wall, because it is the moving part of the fault.

The Fault throw model shown in Fig. 8a and b along the fault plane F4 and F5 was analyzed and some significant deduction has been made: the fault plane in the study area has generally low throw profile denoted with purple colour on the fault throw model while some other portion of the fault planes indicates moderately high throw distributions denoted with blue colour which is evident in the central part of fault F4 and at the western part of fault F5 on the fault throw model.

This implies that in fault dependent traps, this lateral variation in fault displacement is a key factor as fault displacement and its rate of

change controls structural hydrocarbon contacts and column height.

4.2.2 Juxtaposition Map

Reservoir juxtaposition signifies first order seal integrity assessment. Therefore, When considering fault seal analysis it is crucial to look across the faults, in order to achieve this, Juxtaposition maps were generated, and the stratigraphy along the fault planes were made visible. Hence, fault sealing properties are controlled by the juxtaposition of reservoir against sealing lithologies, [31].

The juxtaposition diagram in Fig. 9 was analyzed using the intersection window on petrel 2017 software. Fig. 9 shows the juxtaposition display of facies long the fault planes which is founded on the stochastically simulated facies model based on this, the juxtaposition maps were carefully analyzed. The region on the fault surfaces denoted with yellow colour shows sand lithology while the regions in brown indicates Shale lithology on the fault juxtaposition map.

4.2.3 Shale Gouge Ratio Models

A more precise way of estimating the leakage potential is the derivation of the Shale Gouge ratio. The SGR was calculated based on equation (1) and was estimated by considering the thickness of the bed, average volume of shale from the hanging wall and the footwall.

However, the shale gouge ratio model in Fig. 10a and b has been colour-coded. Leaking fault (Purple colour), poor sealing (blue -Green colour), moderate sealing (green-orange colour) and sealing fault (red colour). The horizon intersections on the shale Gouge Ratio Model reveals the horizons mapped are in the poorly sealing category, this was further confirmed by manually estimating the shale gouge ratio. by carefully analyzing the juxtaposition map.

Therefore, the following variables were determined; volume of shale, throw, bed-thickness, the throw less than 1 meter was not considered as shown in Table 1. The analysis also reveals that none of the reservoirs mapped are in the leaking category. This justifies the fact that this reservoirs are filled with hydrocarbons.

4.2.4 Volume of shale

Volume of shale is derived directly from gamma ray log which is not necessarily the exact volumetric clay content of the rock. The key hypothesis here is that sand and shale material are embedded into the fault gouge in the same proportions as they occur within the wall rocks of the slipped interval.

An accurate determination of the volume of shale from the log data is crucial in predicting whether or not all parts of the fault plane is sealing in terms of Juxtaposition and Shale Gouge Ratio. Fig. 11 shows a direct relationship between the estimated volume of Shale and the shale gouge ratio.

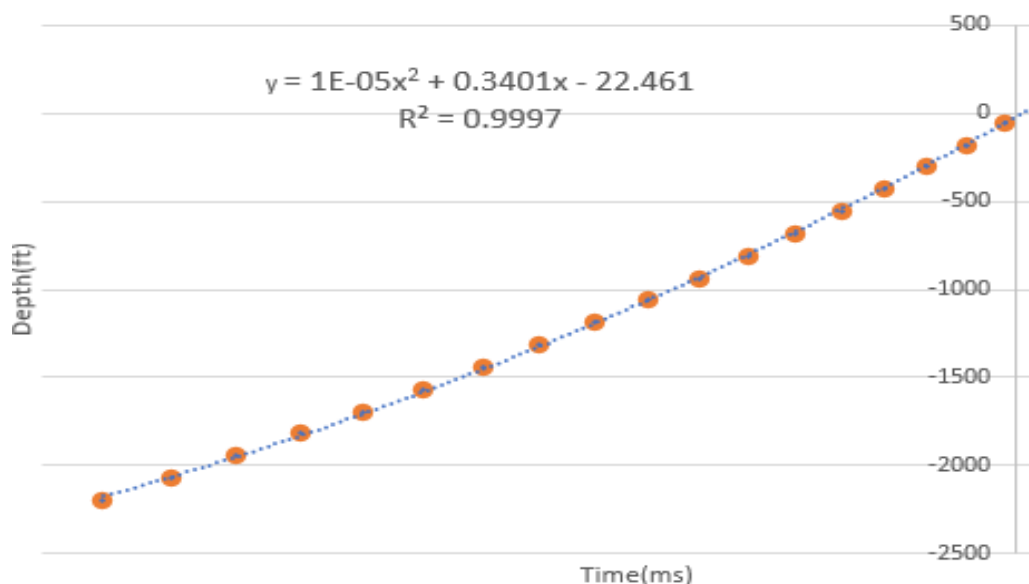


Fig. 6. Time – Depth Relationship curve

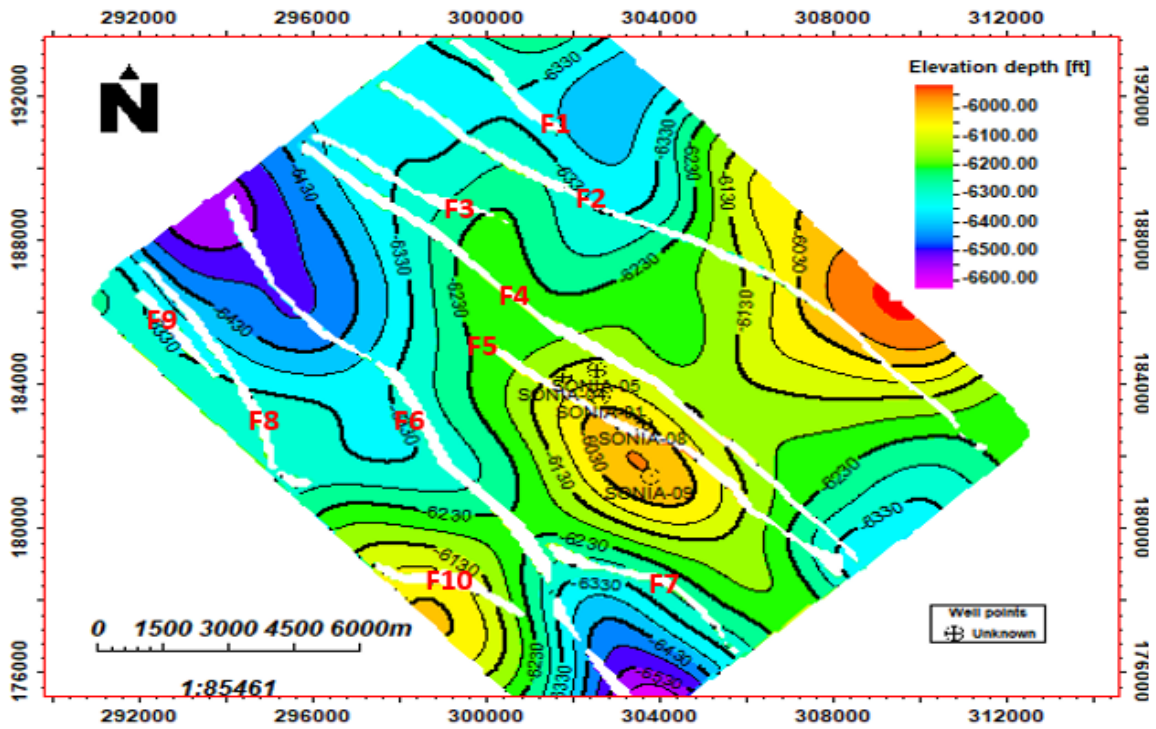


Fig. 7a. Depth Map of Reservoir 1

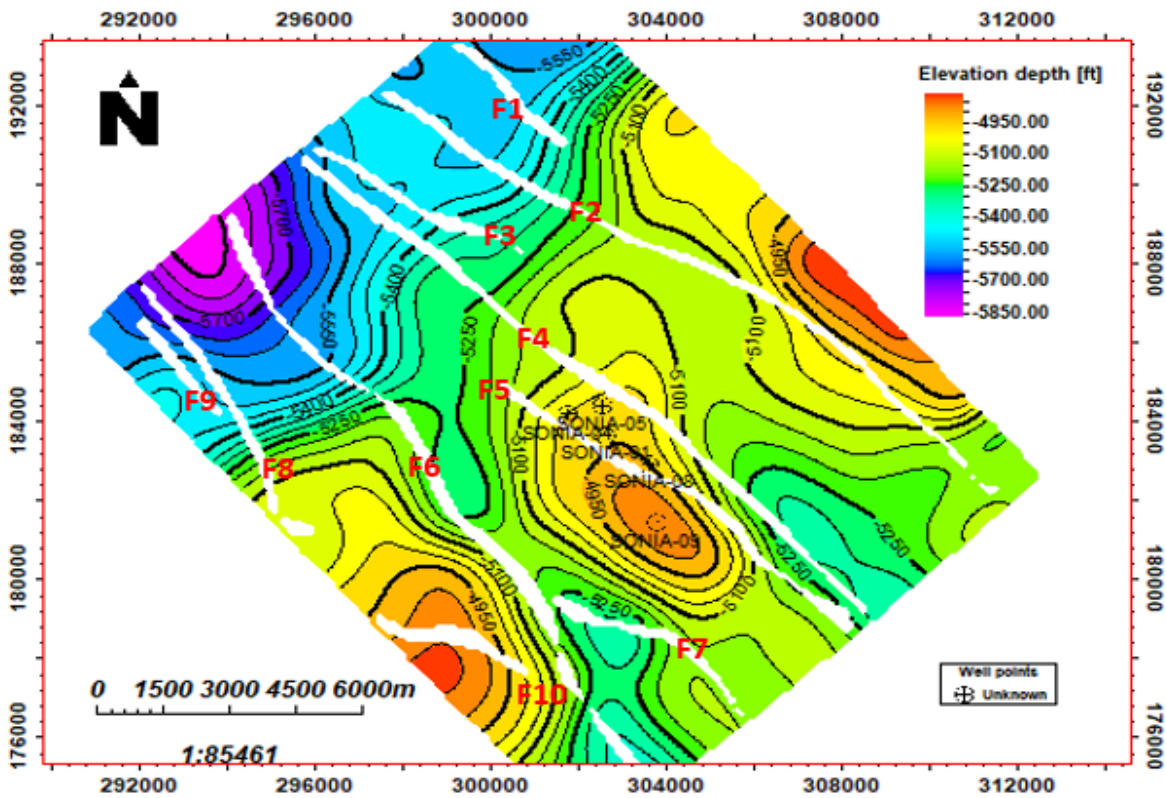


Fig. 7b. Depth Map of Reservoir 2

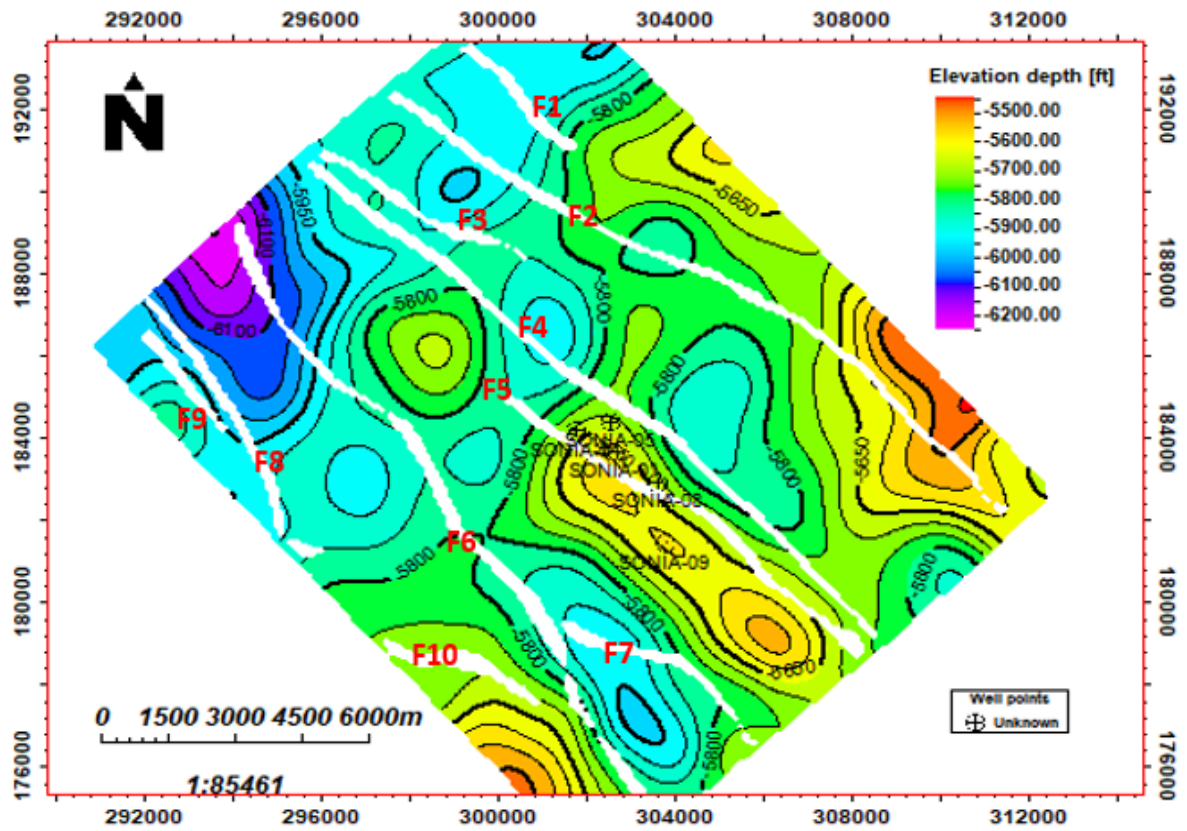


Fig. 7c. Depth Map of Reservoir 3

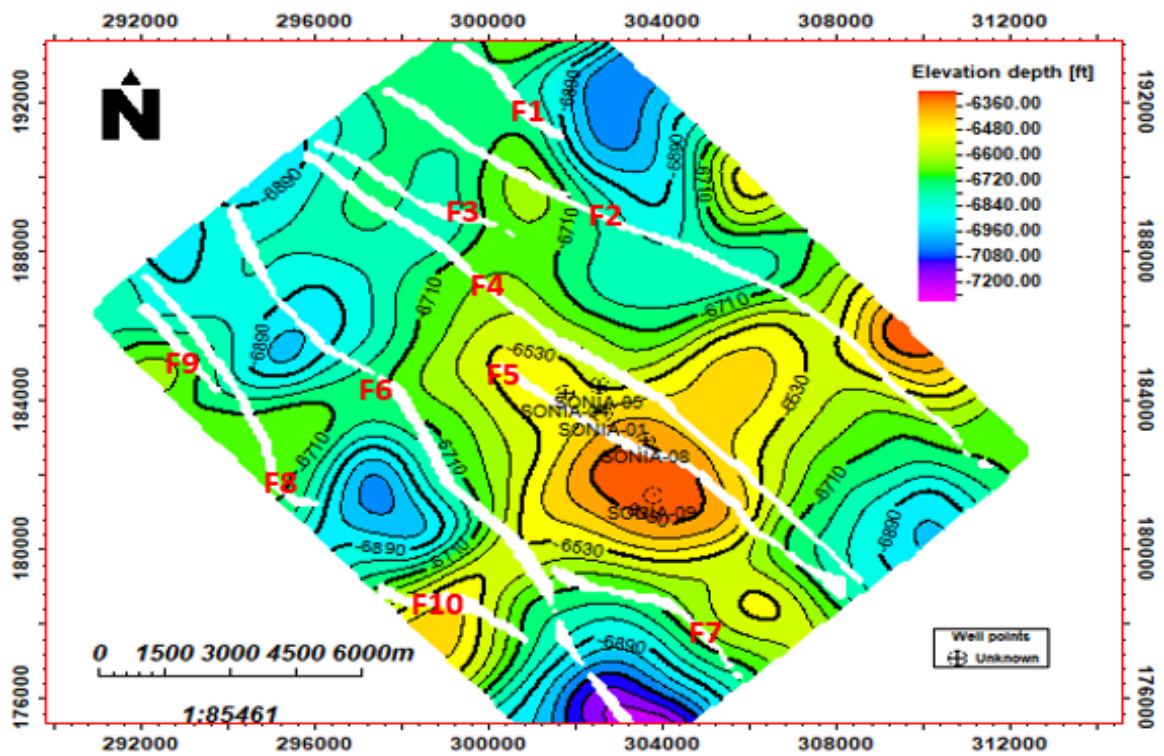


Fig. 7d. Depth Map of Reservoir 4

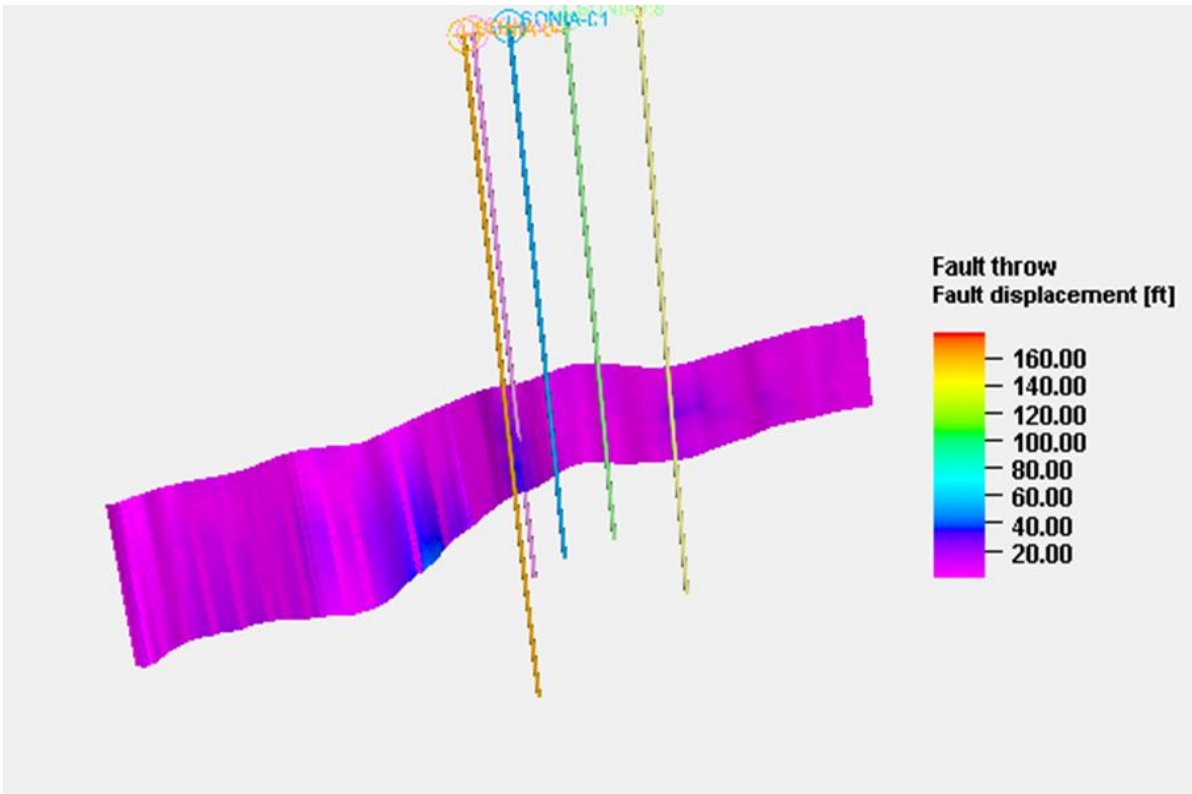


Fig. 8a. Fault Throwing Model of F4

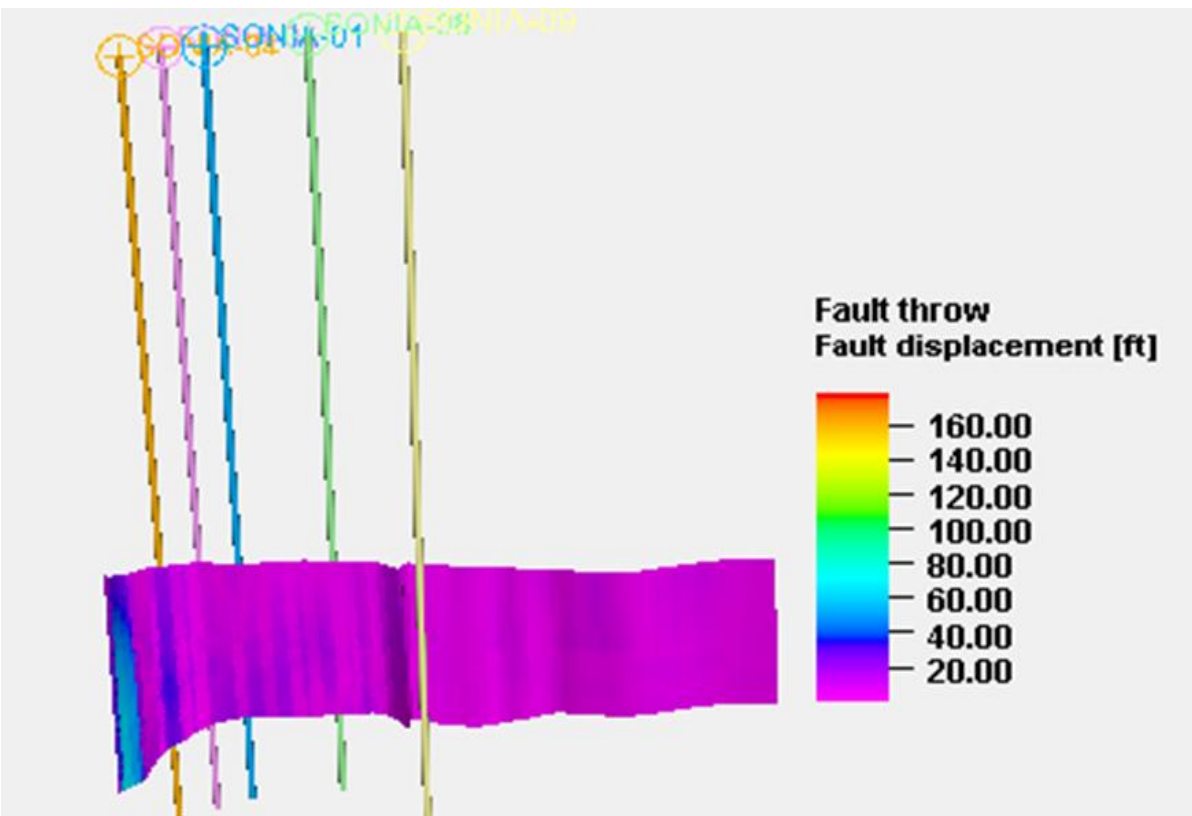


Fig. 8b. Fault Throwing Model of F5

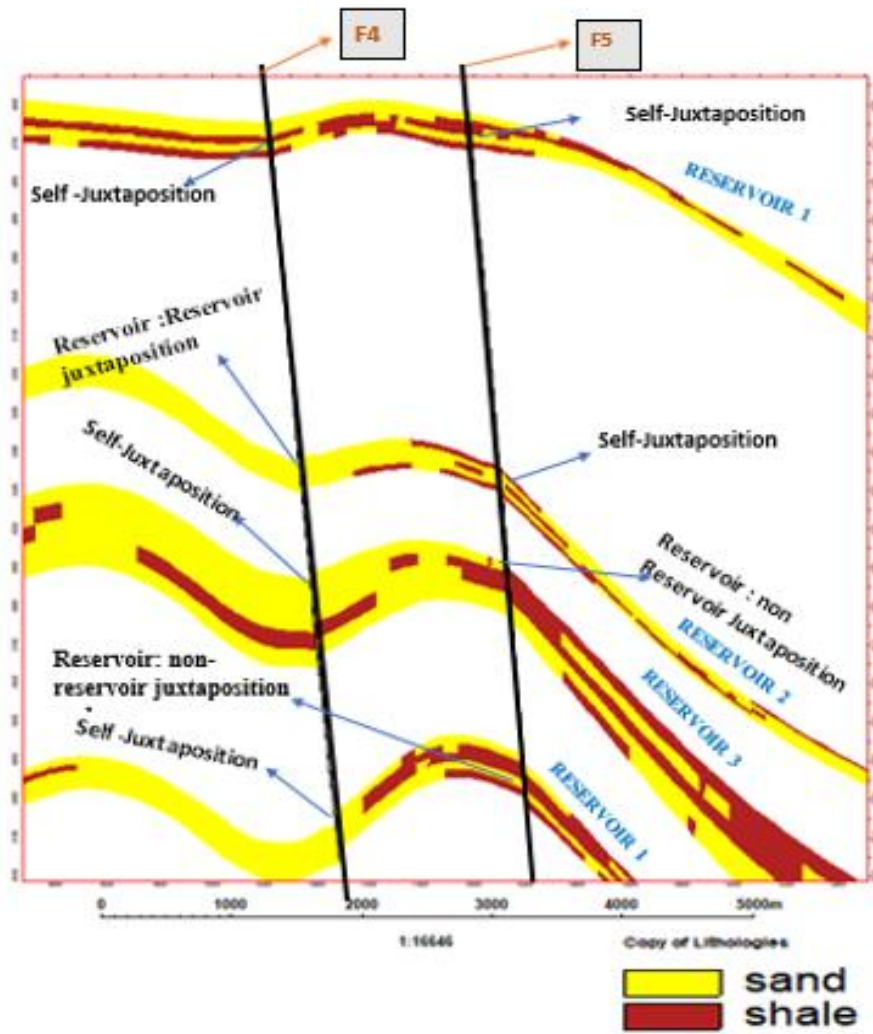


Fig. 9. Juxtaposition Map of fault F4 and F5

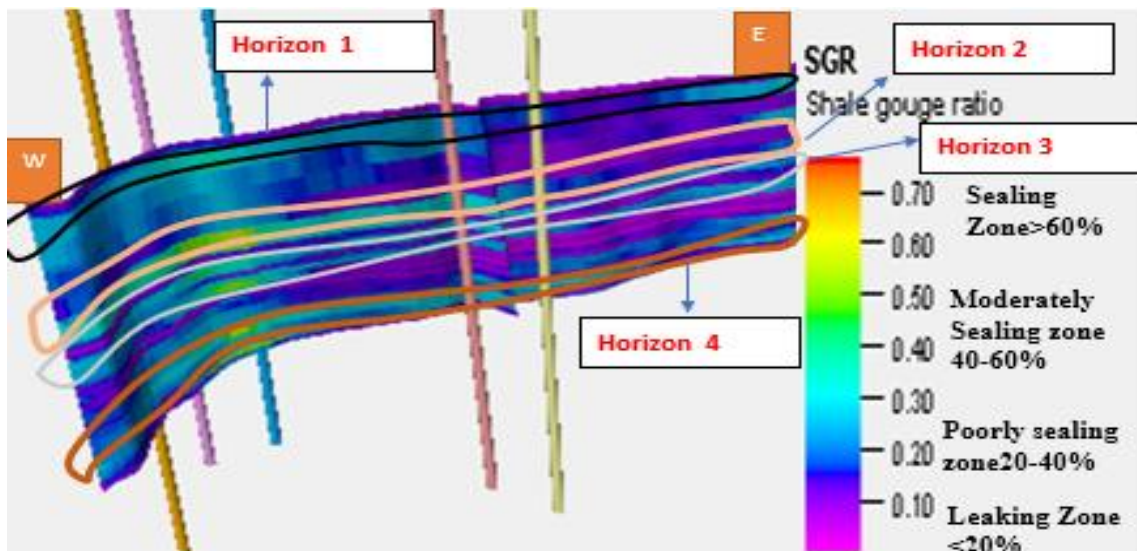


Fig. 10a. Horizon to Fault Intersection on the SGR Model of Fault F4

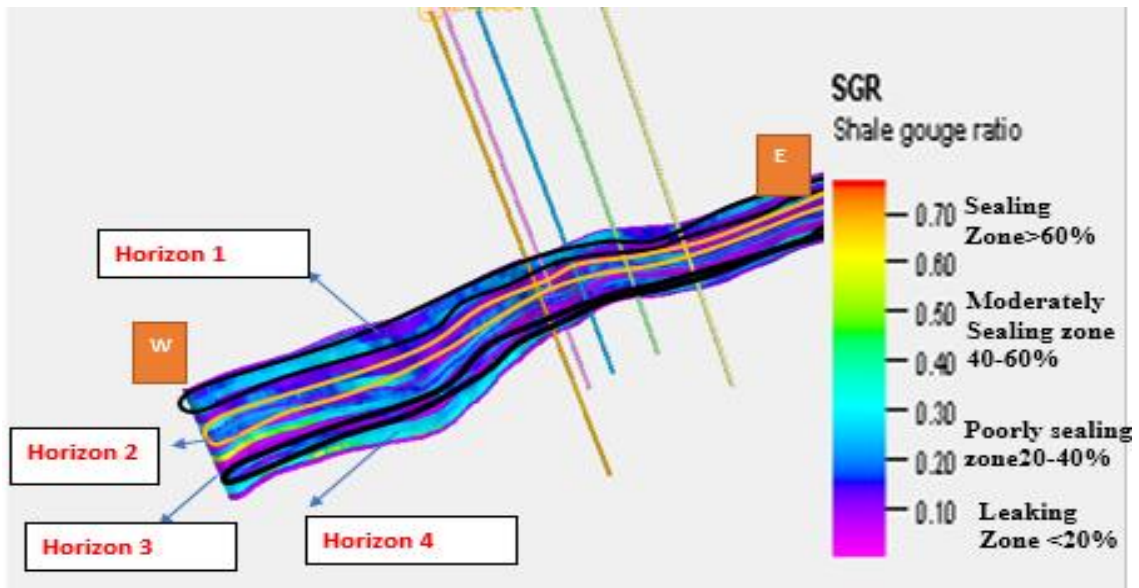


Fig. 10b. Horizon to fault intersection on the SGR Model of Fault 5

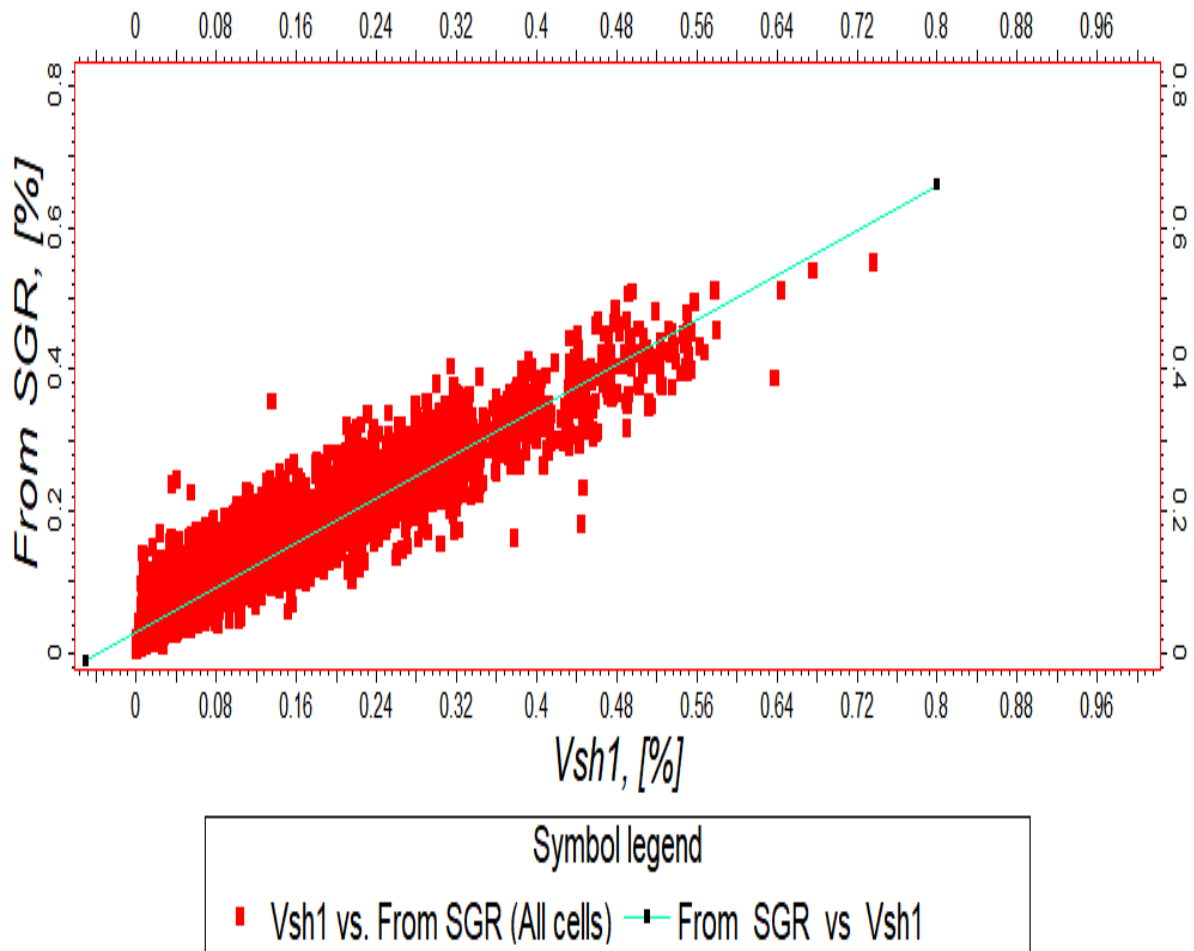


Fig. 11. Plot of Shale Gouge Ratio Versus Volume of Shale

Table 1. Estimated Fault Sealing Properties

Fault/Reservoir	Throw	Bed thickness	Volume of shale	SGR	Fault sealing material
F4 R1	3.1	Sand:3.1	0.13	0.13	Cataclasis
F4 R2	22	Sand 22	0.18	0.18	Cataclasis
F4 R3	16.2	Sand:16.2	0.20	0.20	Phyllosilicate
F4 R4	28	Sand17.4	Vsh1:20	0.24	Phyllosilicate
F5 R1	-	-	-	-	-
F5 R2	1.9	Shale:1.9	0.25	0.25	Phyllosilicate
F5 R3	11.7	Shale:11.7	0.22	0.25	Phyllosilicate
F5 R4	19	Sand :19	0.20	0.20	Phyllosilicate

Table 2. Estimated SGR, FZP and HCH

FAULTS/RESEVOIRS	SGR%	FZP(Psi)	HCH (M)
F4 RES 1	13	14.66	25.91
F4 RES 2	18	14.73	25.91
F4 RES 3	20	14.75	25.95
F4 RES 4	24	14.80	26.04
F5 RES 1	-	-	-
F5 RES 2	25	14.82	26.70
F5 RES 3	25	14.82	26.70
F5 RES 4	20	14.75	25.95

*FZP= Fault Zone Capillary pressure
HCH= Hydrocarbon Column Height*

4.2.5 Hydrocarbon Column Height Models

The hydrocarbon column height models were generated using one of the fault seal algorithms i.e. SGR. The precision of the HCH is dependent on the three dimensional mapping of the reservoir geometry in the vicinity of the fault and the inputs considered in generating the geologic models.

The Predicted column height in which faults in the study area can support ranges between 26.6 m to 28 m as shown in Fig. 12a and b. Therefore, it is interesting to know that the highest predicted column height indicated by orange color corresponds to regions on the fault surface with high SGR values, the reverse is also true, the lowest column height are seen to be purple colour.

This analysis shows that the fault can only support a small column of hydrocarbon before it starts to leak , a direct relationship exist between the shale gouge ratio and hydrocarbon column height. Table 2 shows the estimated fault zone capillary entry pressure and the hydrocarbon column height, based on equation 2 and 8 respectively, which was manually estimated based on the values derived from the shale

gouge ratio that was computed by carefully analyzing the juxtaposition map.

The result from this table reveals a direct relationship between the SGR with fault zone capillary entry pressure and hydrocarbon column height (HCH). The fault zone capillary entry pressure (FZP) and hydrocarbon column height increases with shale gouge ratio.

4.2.6 Fault permeability model

The SGR distribution on a fault plane was then used as an input to generate maps of the fault zone permeability. The wells utilized in this study are targeted within faults F5 and F4. Further analysis needs to be done to understand the flow properties of these faults.

The permeability model for fault F5 and F4 as shown in Fig. 13a and b reveals that the permeability is moderately high i.e. >1mD at the eastern part of the fault, it thus reveal that the materials filling the fault gouge are permeable and it signifies a potential leak. While the western region shows a relatively low permeability i.e. < 1mD, this implies that the material filling the fault gouge is less permeable, signifying a potential seal in that region. Permeability has a

strong correlation with the fault clay content (SGR) with higher clay contents corresponding to low permeabilities as depicted in Fig. 14.

4.2.7 Fault Transmissibility Model

Fig. 15a and b shows the modeled fault transmissibility multipliers (TMs) for Faults F4 and F5. The transmissibility model values were modeled based on the combination of fault rock

permeabilities and thicknesses coupled with the grid cell sizes of the geo-cellular model.

The green colour indicates fault transmissibility values ranging from 0 - 0.10. It signifies potentially sealing zones on the fault plane while the red colour code indicate relatively high transmissibility values which indicates possible leaking zones along the fault plane. Fig. 16 shows direct relationship exist between fault transmissibility and fault permeability.

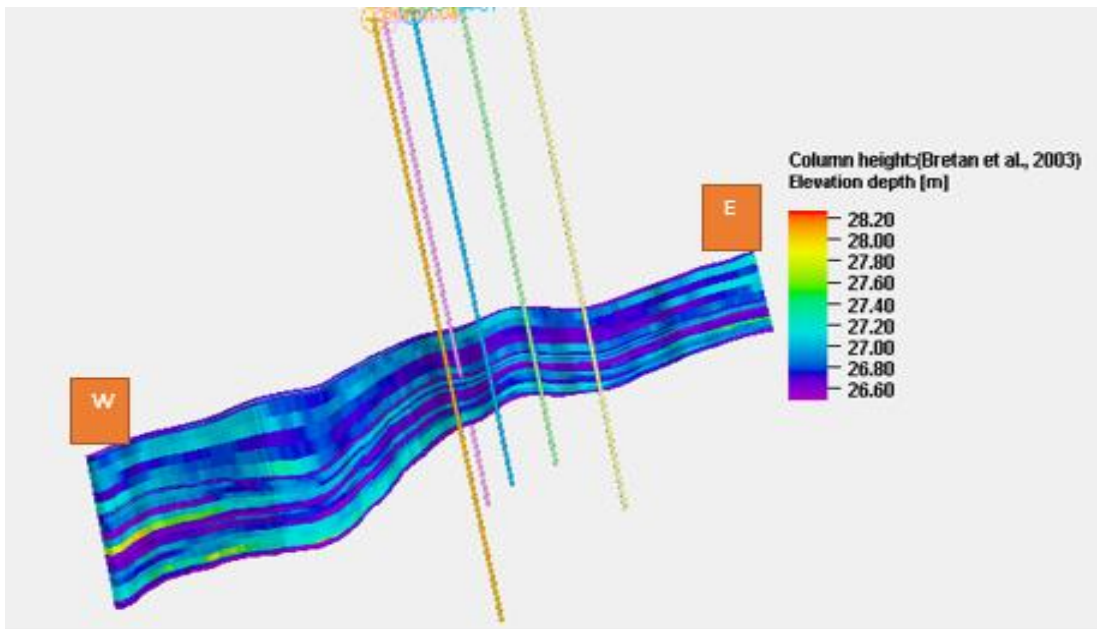


Fig. 12a. Hydrocarbon Column Height Model of Fault 4

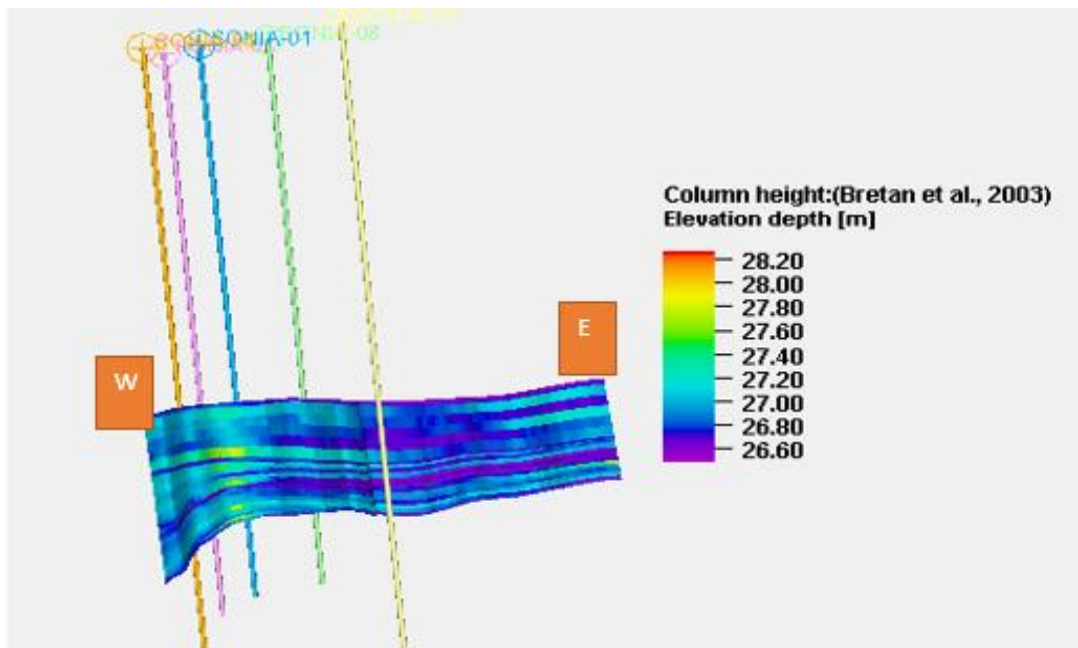


Fig. 12b. Hydrocarbon Column Height Model Of Fault 5

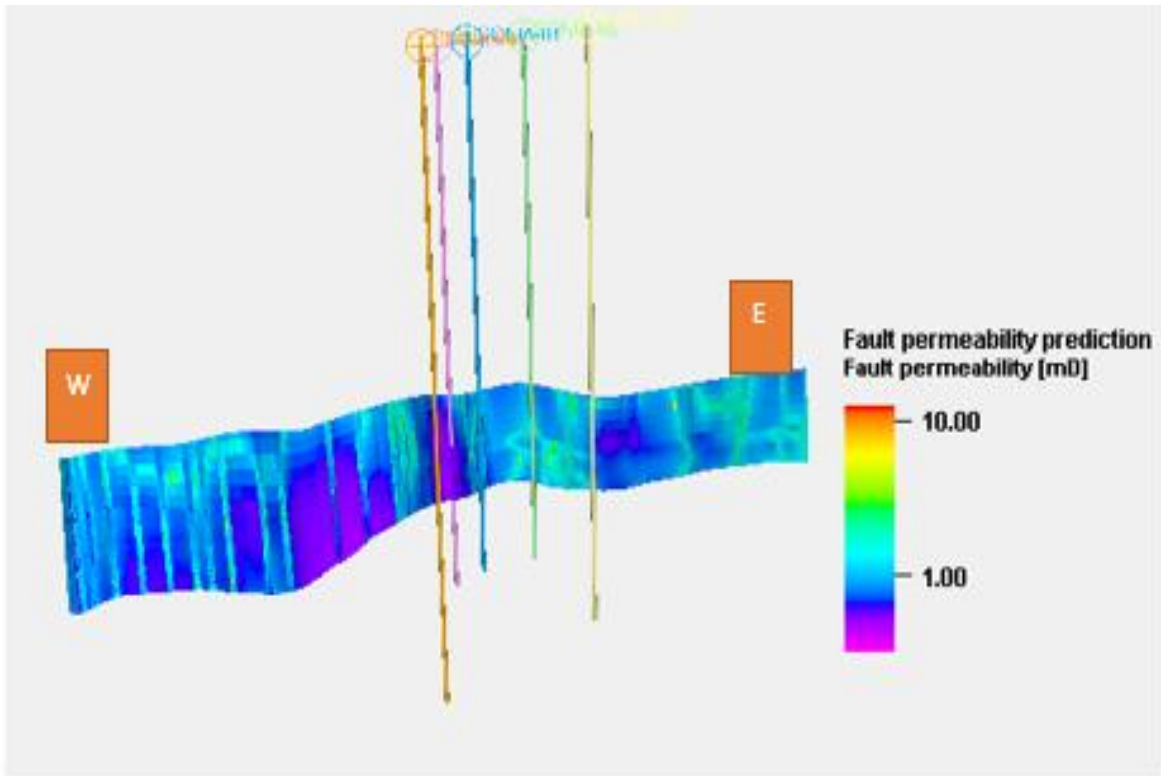


Fig. 13a. Fault Permeability Prediction Model of Fault F4

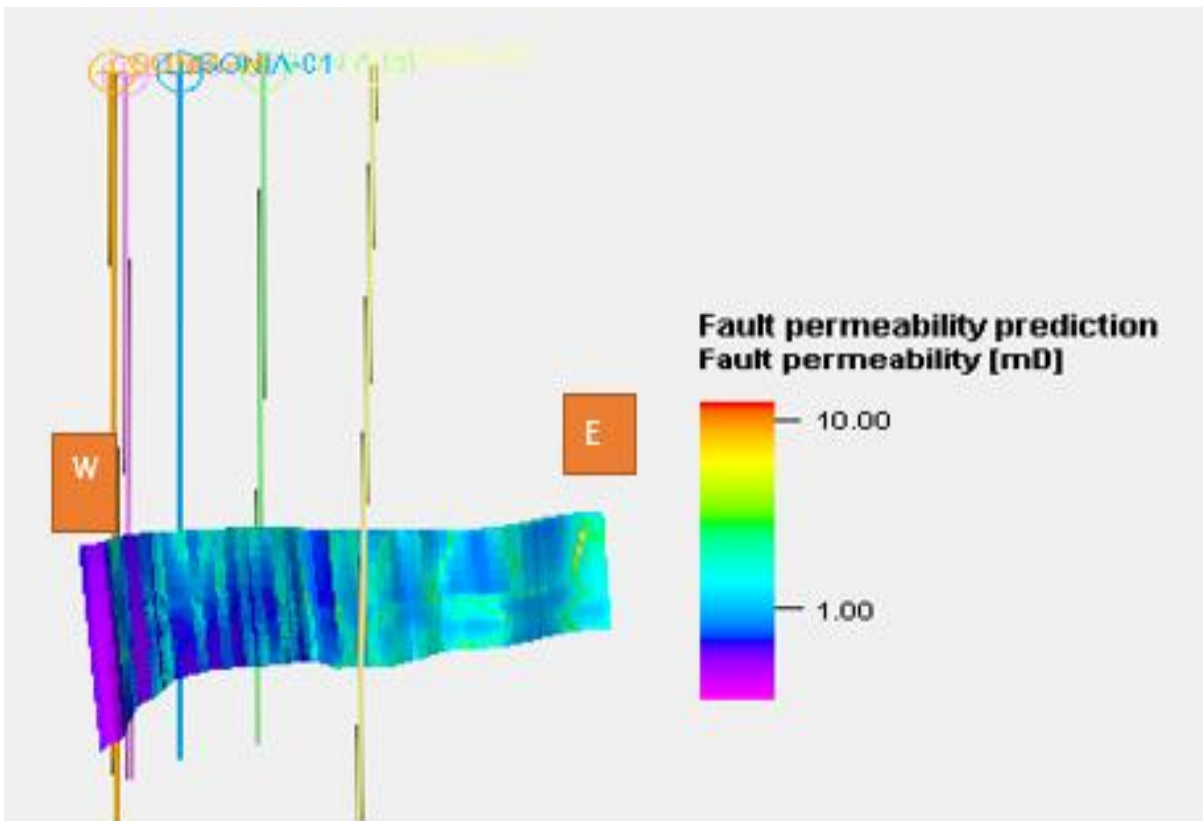


Fig. 13b. Fault Permeability Prediction Model Of Fault F5

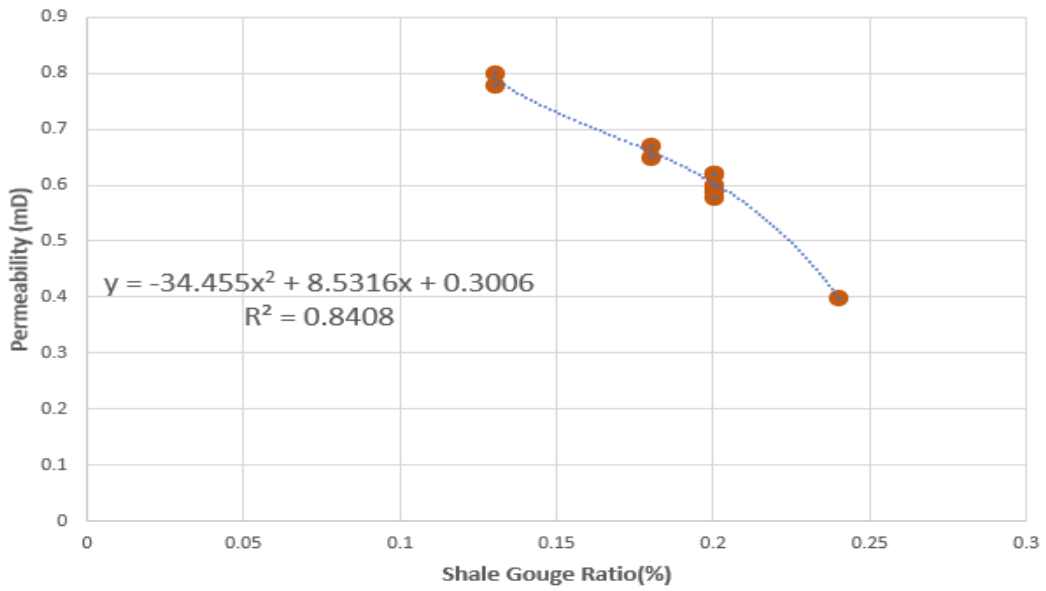


Fig. 14. A plot of shale gouge ratio against permeability

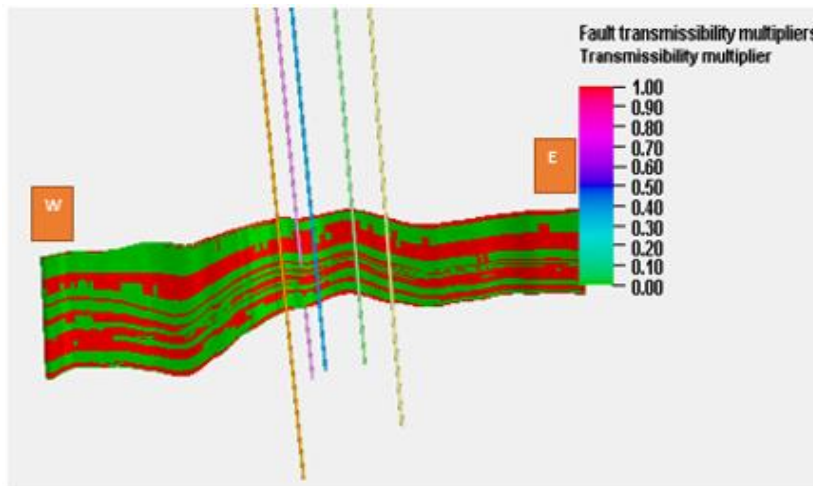


Fig. 15a. Fault Transmissibility Model Of Fault F4

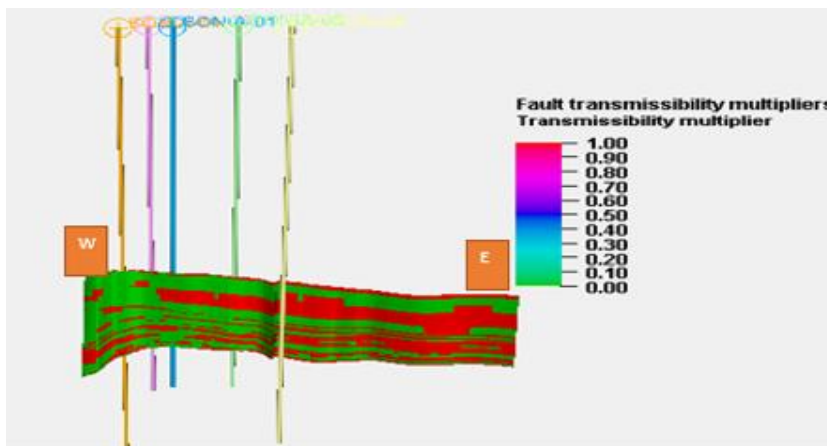


Fig. 15b. Fault Transmissibility Model Of Fault F5

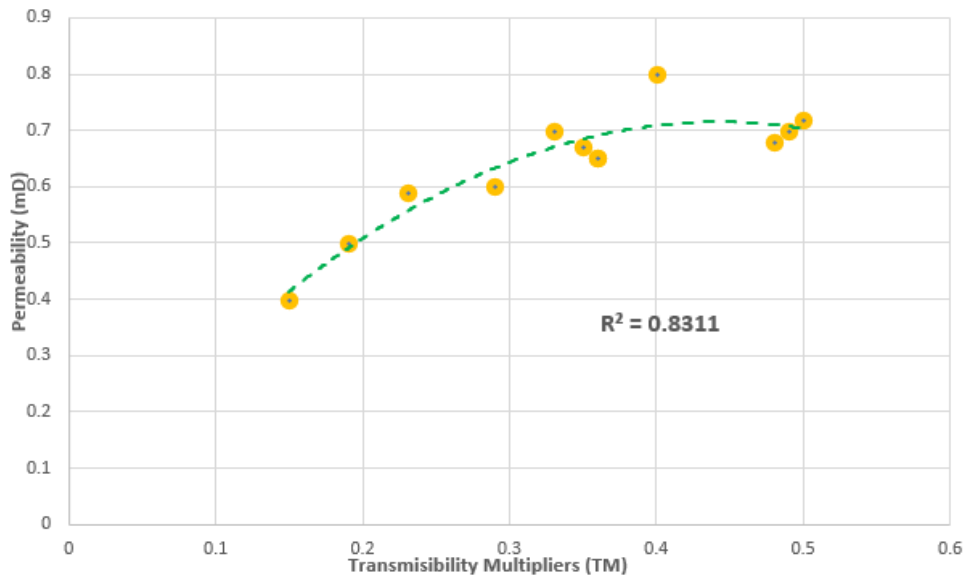


Fig. 16. A plot of fault permeability against fault transmissibility

5. CONCLUSION

The seal integrity of Sonia field has been evaluated in this study. The juxtaposition map has shown the regions within the reservoirs with potential cross fault leak i.e. by indication on the fault surfaces regions of sand against sand lithologies. Discovered on the SGR models was that, on the fault plane the none hydrocarbon bearing horizons fall within the leaking zone (purple colour) while most of the hydrocarbon bearing horizons are supported by poor sealing zones i.e. SGR range of 20% to 40%.

From the Hydrocarbon Column Height (HCH) model, a column height ranging from 26.6m to 28.0m was observed within the fault planes. This implies that the fault can only support a small column for hydrocarbon accumulation before it starts to leak. The result of permeability model of the faults shows that in some regions the permeability is less than 1mD along the fault plane with corresponding transmissibility values ranging between 0 and 0.2. The implication was that these regions along the faults planes are closed (sealed) and might eventually prevent migration of fluid out of the reservoir while regions with transmissibility values of 1 were interpreted as open zones.

COMPETING INTERESTS

Authors have declared that no competing interests exist.

REFERENCES

1. Yangwen Pei, Paton DA, Knipe RJ, Kongyou Wu. A review of fault sealing behavior and its evaluation in siliciclastic rocks Earth-Science. 2015;150: 121–138.
2. Ogilvie SR, Dee SJ, Wilson RW, Bailey WR. (eds) Integrated Fault Seal Analysis. Geological Society, London, Special Publications. 2020;496:1–8.
3. Cervený K, Davies R, Dudley G, Fox R, Kaufman P, Knipe RJ, Krantz B. Reducing uncertainty with Fault-Seal Analysis. Oilfield Review. 2004;16(4): 38-51.
4. Yielding G. Shale Gouge Ratio-Calibration by Geo-history, in A.G. Koestler and R. Hunsdale, Hydrocarbon Seal Quantification, Norwegian Petroleum Society Special Publication. 2002;11:109-125.
5. Irving AD, Chavanne E, Faure V, Buffet P, Barber E. An uncertainty modelling workflow for structurally compartmentalized reservoirs, Geological Society, London, Special Publications 2010;347:283 – 299
6. Smith DA. Theoretical consideration of sealing and non-sealing faults. American Association of Petroleum Geologists Bulletin. 1966;50:36-3374,
7. Schowalter TT. Prediction of caprock seal capacity. AAPG, 1981;65:987–988.

8. Yielding G, Bretan P, Freeman B. Fault Seal Calibration: a brief review. Geological Society, London, Special Publications. 2010;347:243–255.
9. Eshimokhai S, Akhirevbulu OE. Reservoir characterization using seismic and well logs data (a case study of Niger Delta). *Ethiop. J. Environ. Stud. Manag.* 5 (Suppl. 2) 2012;302-504.
10. Oyedele KF, Ogagarue DO, Mohammed DU. Integration of 3D seismic and well log Data in the optimal reservoir characterization of EMI field, offshore Niger Delta oil province, Nigeria. *Am. J. Sci. Ind. Res.* 2013;4(1):11e21.
11. Oyeyemi KD, Aizebeokhai AP. Hydrocarbon trapping mechanism and petrophysical analysis of afam field, offshore Nigeria. *Int. J. Phys. Sci.* 2015;10(7):222e238.
12. Whiteman AJ. Nigeria: Its Petroleum Geology, Resources and Potential, Graham and Trotman, London. 1982;12-15
13. Haack RC, Sundaraman P, Diedjomahor JO. Niger Delta petroleum systems, Nigeria in Petroleum Systems of South Atlantic Margins, M. R. Mello and B. J. Katz, Eds. American Association of Petroleum Geologists Memoir. 2000; 73:213–231.
14. Doust H, Omatsola E. Niger-Delta. Divergent/passive margins basins AAPG memoir Bulletin. 1990;75:162-1643.
15. Short K, Stuble. Outline of Geology of the Niger delta,” The American Association of Petroleum Geologists Bulletin. 1967; 51:761–779,
16. Avbovbo AA. Tertiary lithostratigraphy of Niger Delta,” The American Association of Petroleum Geologists Bulletin. 1978;62: 295–300.
17. Lawrence SR, Munday S, Bray R. Regional geology and geophysics of the eastern Gulf of Guinea (Niger Delta to RioMuni),” The Leading Edge. 2017; 21(11):1112–1117.
18. Evamy BD, Haremboure J, Knaap WA, Molly FA, Rowlands PH, Kamerling P. Hydrocarbon habitat of tertiary Niger Delta American Association of Petroleum Geologist Bullrtin. 1978;62(1):1-39.
19. Dim CIP. Hydrocarbon Perspectivity in the Eastern Coastal Swamp Depo-belt of the Niger Delta Basin–Stratigraphic Framework and Structural Styles,” in Springer Briefs in Earth Sciences. 2017; 105 -150
20. Lawal, Wasiu. Fault seal analysis a method to reduce uncertainty in hydrocarbon exploration: case study of moyo field Niger Delta basin. In: A Paper Presented at Dharmattan Nigeria Limited General Meeting 2015:135-155
21. Yielding GB, Freeman, Needham DT. Quantitative Fault Seal Prediction. AAPG Bulletin. 1997; 81(6):897-917-811.
22. Sahoo TR, Tuser R, Nayak S, Sankar S, Senapati S, Singh YN. Fault seal analysis: a method to reduce uncertainty in hydrocarbon exploration, Case study: northern part of Cambay Basin, 8th Biennial International Conference and Exposition on Petroleum Geophysics. 2015;1–9 .
23. Bretan P, Yielding G, Jones H. Using calibrated shale gouge ratio to estimate hydrocarbon column heights. American Association of Petroleum Geologists Bulletin, 2003;87:397–413.
24. Berg RR. Capillary pressures in stratigraphic traps’, American Association of Petroleum Geologists Bulletin, 1975;59(6):939-956.
25. Schowalter TT. Mechanics of secondary hydrocarbon migration and entrapment’ ,American Association of Petroleum Geologists Bulletin. 1997;63(5):723-760.
26. Watts NL. Theoretical aspects of cap-rock and fault seals for single and two-phase hydrocarbon columns’, *Marine and Petroleum Geology.* 1987;4(4):274-307.
27. Ingram GM, Urai JL, Naylor MA. Sealing processes and top seal assessment. *Nor. Pet. Soc. (NPF) Spec. Publ.* 1997;7 (165e174):67-70
28. Sperrevik, S., Gillespie, P.A., Fisher, Q.J., Halvorsen, T. and Knipe, R.J. ‘Empirical estimation of fault rock properties. In: Koestler, A. G. & Hunsdale, R. (Eds.), ‘Hydrocarbon Seal Quantification’, Norwegian Petroleum Society, Special Publication, Elsevier, Singapore. 2002;11: 109–125.
29. Manzocchi T, Walsh JJ, Nell P, Yielding G. Fault transmissibility multipliers for flow simulation models. *Petroleum Geoscience.* 1999;5:53-63.
30. Sunmonu LA, Adabanija MA, Adagunodo TA and Adeniji AA. Reservoir Characterization and by-passed pay analysis of Philus field in Niger Delta, Nigeria: *International Journal of Advanced Geosciences.* 2016;4(2):28-41.

31. Adagunodo TA, Sunmonu LA, Adabanija MA. Reservoir characterization and seal integrity of Jemir field in Niger-Delta, Nigeria Journal of African Earth Sciences. 2017;129-791.

© 2021 Raymond and Amigun; This is an Open Access article distributed under the terms of the Creative Commons Attribution License (<http://creativecommons.org/licenses/by/4.0>), which permits unrestricted use, distribution, and reproduction in any medium, provided the original work is properly cited.

Peer-review history:
The peer review history for this paper can be accessed here:
<https://www.sdiarticle4.com/review-history/74042>